10th International Heat Transfer Conference, Brighton, England, 14-18 August 1994

EXPERIMENTAL AND NUMERICAL STUDY OF THREE-DIMENSIONAL NATURAL CONVECTION AND FREEZING IN WATER

C. Abegg[1], G. de Vahl Davis[2], W.J. Hiller[1], St. Koch[1],
T.A. Kowalewski[1*] E. Leonardi[2] and G.H. Yeoh[2]

[1]Max-Planck-Institut für Strömungsforschung, D-37073 Göttingen
[2]University of New South Wales, Kensington, 2033 Australia

ABSTRACT

In this paper we describe an experimental and numerical investigation of the response of an initially isothermal fluid in a cubical box to an instantaneous cooling of the upper surface of the box. The other five surfaces are neither adiabatic nor ideal heat conductors. When the lid temperature drops below $0^{\circ}C$, ice begins to form on the top wall. The onset of convection in such a problem was investigated and the effects of the ice interface on the convection are presented. The importance of the thermal boundary conditions on the flow structure is also discussed.

1. INTRODUCTION

The aim of this investigation is to explore both experimentally and numerically the transient development of convective flow in a cubical cavity with a cooled lid. The effect of phase change at the cooled lid is of special interest. Due to the freezing, a new upper boundary of the liquid region is created and grows; how this modifies the flow pattern has been investigated.

The occurrence of convective flow in the presence of vertical temperature gradients has been extensively studied analytically, computationally and experimentally for shallow cavities with isothermal, adiabatic or infinitely extended side walls; this is known as the Rayleigh-Bénard problem. Such a flow, with a characteristic periodic, two-dimensional structure, is usually stable only within a relatively narrow range of Rayleigh number ($1700 < Ra < 10000$). In a bounded domain the flow becomes highly three-dimensional, with complicated cross-roll structures (Stella *et al.* 1993), and its stability range may increase up to $Ra \approx 10^5$.

In our experiments on a lid-cooled cavity, the other five walls are not truly either isothermal or adiabatic; there was heat flux into the liquid through the sides and bottom, as well as heat flux out through the lid, which were responsible for the generation of the flow. An attempt was therefore made in our computations to model this 'leakage' of heat into the test fluid.

*On leave of absence from the Institute of Fundamental Technological Research, Polish Academy of Sciences, PL 00-049 Warszawa

It has been found that these boundary conditions have a stabilising effect on the overall flow. In our present experimental and numerical investigations we find that stable flow structures are possible at $Ra > 10^6$, well above the second critical number for the Rayleigh-Bénard instability. Starting from a uniform temperature, the transient behaviour of the flow has, in addition to the characteristic axisymmetrical flow at the start and at the final state, several intermediate structures with a reverse flow direction and a completely chaotic flow pattern. When phase change takes place, in our case freezing on a lid surface, both the thermal and kinematic boundary conditions change. This is an additional non-linear coupling complicating the predictions of the flow patterns. Despite the fact that freezing starts at a planar surface, the ice interface does not remain planar. Its distortion in turn affects the convection in the whole cavity. A complex interaction between the flow, the moving boundary and the latent heat removed at the solid/liquid interface determines the flow pattern which is established.

The problem of melt-flow in a lid-cooled cavity has a practical application in a number of manufacturing processes and physical situations. A large scale example is the freezing of water reservoirs, where at night, cooling from above initiates freezing and generates convective flow beneath the ice. On a smaller scale, it has been recognized among crystal growers that the flow pattern beneath the solidifying surface is of critical importance to crystal quality. For example, when a crystal is grown in directional solidification from a melt with alloyed impurities, their distribution will affect the process of impurity diffusion in the melt as well as in the solid (Rosenberger & Müller 1983, Müller *et al.* 1987).

2. FORMULATION OF THE PROBLEM

We consider the convective flow in a cubical box filled with a viscous heat conducting liquid, which in this case is water. The fluid density is temperature dependent. In some of our studies viscosity, thermal conductivity and heat capacity were also assumed to be temperature dependent. The flow takes place in a container with an aspect ratio of one. The top surface of the water is isothermal at the temperature T_c, which is assumed to be equal to the lid

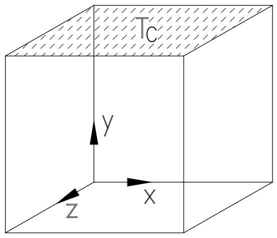

Figure 1: *The cubical box with cooled top surface. The y-axis is parallel to the gravity vector $\vec{g}$.*

temperature T_l, except in the case of freezing where it is taken at the ice-water interface temperature of 0^oC. The other five walls are non-adiabatic, allowing the entry of heat from the external fluid - water - which surrounds the cavity (Fig.1).

The temperature of the fluid in the external bath $T_h > T_c$ was kept constant. Due to forced convection in the bath the temperature at the external surfaces of the box was close to T_h. The temperature field at the inner surfaces of the walls adjusted itself depending on both the flow inside the box and the heat flux through and along the walls. The initial fluid temperature and temperature of all six walls was T_h. Convection started when, at time $t = 0$, the lid temperature dropped to T_l.

The two basic dimensionless parameters defining the problem, the Rayleigh number

$$Ra = \frac{g\beta \Delta T H^3}{\kappa\nu} \tag{1}$$

and the Prandtl number

$$Pr = \frac{\nu}{\kappa} \ , \tag{2}$$

are used to characterize and compare the numerical and experimental results.

In the above definitions, g, H, ΔT, κ, β, ν denote respectively the gravitational acceleration, the cavity height, the temperature difference $T_h - T_c$, the thermal diffusivity, the coefficient of thermal expansion and the kinematic viscosity. The non-dimensional temperature is defined as: $\theta = (T - T_c)/\Delta T$.

For the freezing problem, the Stefan number also becomes one of the important flow parameters:

$$Ste = \frac{c_p \Delta T}{L_f}, \tag{3}$$

where c_p, L_f are specific heat and latent heat of fusion, respectively. As these properties for water (the fluid used in our experiments) are practically constant, the important variable in the Stefan number becomes the temperature difference ΔT.

2.1. Numerical models

A numerical simulation of the problem was performed using a finite difference model of the Navier-Stokes and energy equations. Two three-dimensional (3-D) numerical codes have been used: FRECON3D (Goh *et al.* 1988), which is a false transient solver for all studies of steady convection of a constant property fluid, and ICE3D (Yeoh 1993), a code developed to study transient convection with phase change in a fluid with temperature-dependent properties. The vorticity-vector potential formulation (Mallinson & de Vahl Davis 1977) is used in both codes.

When variable properties are used, the conventional non-dimensional approach does not provide any significant advantage since the boundary properties, that is temperatures and all dimensions, can either be calculated from the non-dimensional numbers or have to be used as boundary conditions in order to fully specify the problem (Leonardi & Reizes 1981). However, for ease of comparisons with other results, the use of a non-dimensional approach has been retained in the variable properties code ICE3D. Their values are calculated at a reference temperature, which in our case was the top surface temperature T_c.

When phase change takes place, the movement of the solid-liquid interface is computed with the use of an energy balance at the interface which incorporates the latent energy transfer accompanying phase change. As the physical domain changes in shape, the interface boundary grid must be generated at each time step, following which a new computational grid is determined in the liquid and solid regions.

Independent conservation equations are solved for each phase and are coupled by the condition at the solid-liquid interface. Transformation techniques were used to map the moving physical domain onto the computational domain.

When simulating experimental conditions, the main problem which arises is the proper definition of thermal boundary conditions (TBC). In each of our codes, the TBC are sufficiently flexible to allow the imposition of an arbitrary temperature, a specified heat flux or a specified heat transfer coefficient on each of the six surfaces of the box. In the present study the horizontal top wall was assumed to be isothermal. On the remaining walls, which were not strictly either adiabatic or isothermal, the convective TBC were calculated assuming one dimensional heat conduction through each wall. This was estimated by using heat transfer theory applied to a thick, infinitely wide plane plate of uniform conductivity exchanging heat with an external unlimited environment. The non-dimensional condition for the temperature θ at the inner boundary can be written in the general form as

$$a\theta + b\frac{\partial \theta}{\partial n} = c \tag{4}$$

The constants a, b and c can be varied to specify the boundary condition existing in the simulated experiment.

Solutions were obtained using a $61 \times 61 \times 61$ mesh for FRECON3D and a $51 \times 51 \times 51$ mesh for ICE3D.

3. EXPERIMENTAL APPARATUS

The experimental set-up used to acquire temperature and velocity fields consists of the convection box, a xenon flash tube and a CCD colour camera. The box, of 38mm inner dimension, has an isothermal lid made of a black anodized metal and five 8 mm thick plexiglas walls. The lid was maintained at a constant temperature by water

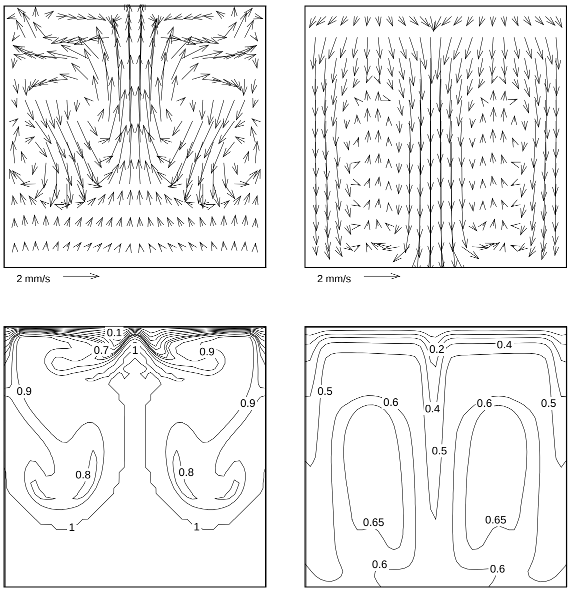

Figure 2: *Onset of convection in the lid-cooled cavity. $Ra = 2.7 \times 10^6$, $Pr = 8$. Numerical simulation for t=40s (left) and t=200s (right). Velocity vectors and non-dimensional temperature at the vertical centre plane z=0.5.*

flowing through internal channels in the metal plate. The temperature of the water cooling the lid and of that in the bath surrounding the five non-adiabatic walls was controlled by thermostats. The temperature at the lid and at a few control points inside the cavity was continuously monitored using thermocouples. Distilled water was used in the experiments.

Two experiments were performed, one without phase change and one with change. The lid was suddenly cooled (in practice, within a time of about 90 seconds) from the initial fluid and surrounding water bath temperature T_h to a temperature of T_l. In experiment 1, without phase change, $T_h = 21^oC$ and $T_l = 15.5^oC$. In experiment 2, in which ice was formed, $T_h = 20^oC$ and $T_l = -10^oC$. In the latter case, the formation of ice on the lid established the solid-liquid interface temperature at 0^oC. Hence, the temperature difference ΔT in the water varied in the experiments from 5.5 to $20K$. The corresponding values of Rayleigh, Prandtl and Stefan numbers for the two experiments were respectively $Ra = 2.7 \times 10^6$ or 3.1×10^6, $Pr = 8$ or 13 and $Ste = 0.252$.

The temperature and velocity fields were measured by means of liquid crystals (LC) suspended as small tracer particles in the liquid. The visualisation of temperature using thermochromic liquid crystals is based on their temperature-dependent reflectivity at the visible light wavelengths. If the liquid crystals are illuminated with white light, then the colour of the light they reflect changes from red to blue when the temperature is raised. This occurs within a well defined temperature range (the so called colour play range), which depends on the type of LC used. The temperature is determined by relating the colour to a temperature calibration function (Hiller *et al.* 1993). Thus by analysing the colour (hue) of the incoming light it is possible to measure quantitatively the temperature distribution in the whole two-dimensional (2-D) cross section of the cavity. Due to the nonlinearity of the hue-temperature relationship, the accuracy of the measurement varies from $\pm 2.5\%$ at the low end to $\pm 8\%$ at the high end of the covered temperature range.

The flow was observed at various vertical and horizontal cross sections of the cavity using a light sheet technique. The xenon flash tube generates a 2 mm thick sheet of white light, which illuminates the selected cross-section of the flow. A three chip CCD colour camera (Sony DXC-750P), which gives an RGB-signal for the red, green and blue components of the incoming light, was used to observe the flow. The images were acquired by three identical 8-bit frame grabbers (PPI- Eltec) in a VME-bus computer.

The 2-D velocity vector distribution has been measured by particle image velocimetry (PIV). The method applied here (Paul 1991) uses two separately captured digital images taken at a constant time interval (typically 5s) to evaluate the motion of the particles. Computer supported evaluation of the mean translation vector for each selected section of the image gives the 2-D velocity distribution in the whole plane of observation. Use of the image processor and liquid crystals as tracer particles allowed simultaneous measurement of the temperature and velocity field of the flow.

To obtain a general view of the flow pattern, several images were recorded periodically within a given time interval and were then superimposed. Displayed images are similar to multiple exposure photographs, showing the flow direction and its structure.

4. RESULTS

Two particular aspects of the flow have been investigated in the experiments: (i) the unsteady development of the flow structure and (ii) the development of the ice front and its interaction with the convective flow structure.

4.1. Onset of convection

When the top wall was suddenly cooled to a temperature of 15.5°C, a cold thermal boundary layer appeared. Within the first 20s it became unstable, breaking down into four symmetrical plumes falling down along the side walls (Fig.2a). This flow, in turn, generated several recirculating zones, transporting heat and vorticity from the side walls to the centre.

After 3-5 minutes a general flow pattern was established (Fig.2b). In the vertical centre plane shown, this consisted of two downward flowing 'jets' of cold liquid along the side walls, and another one along the vertical axis of the box. However this configuration was unstable.

After 5-8 minutes - the time depending on experimental disturbances or numerical noise - a dramatic transformation of the flow structure took place. The central downward flow jet became unstable and meandered around the cavity for approximately 30 minutes. Figures 3 and 4 show

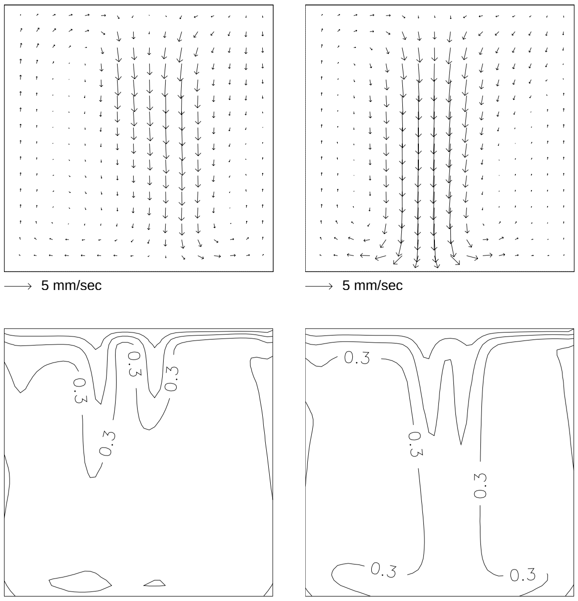

Figure 3: *Numerical simulation of the development of the flow structure.* $Ra = 2.7 \times 10^6$, $T_h = 21°C$, $T_c = 15.5°C$. *Velocity vectors and non-dimensional temperature distribution at the vertical centre plane z=0.5.*

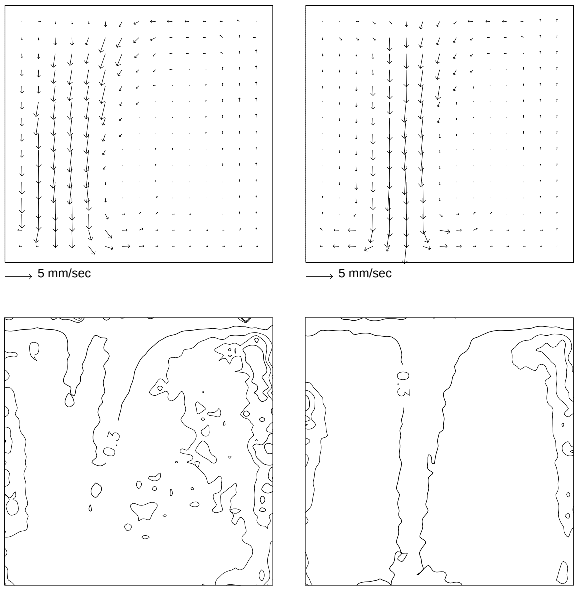

Figure 4: *Measured development of the flow structure.* $Ra = 2.7 \times 10^6$, $T_h = 21°C$, $T_c = 15.5°C$. *Velocity vectors and non-dimensional temperature distribution at the vertical centre plane z=0.5.*

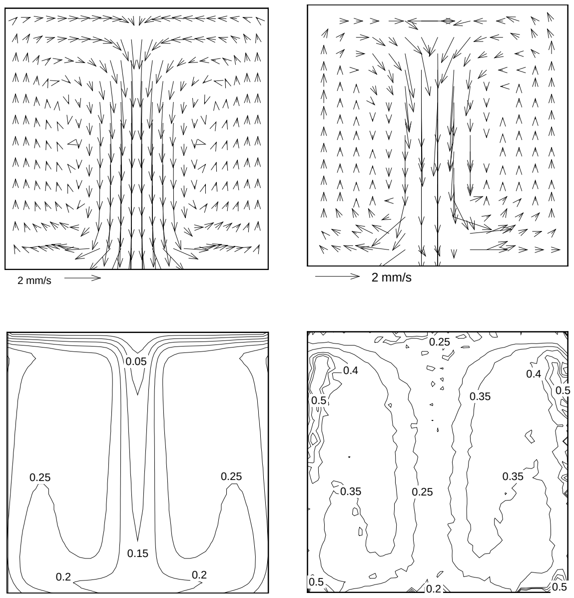

Figure 5: *Convection in the lid-cooled cavity at the vertical symmetry plane z=0.5. Velocity and non-dimensional temperature at the final state (t=60 minutes). Numerical simulation (left); experiment (right).*

the asymmetric swing of the jet from left to right which occurred during this period. After passing through several strongly asymmetrical flow forms a final configuration with a single cold downward flowing jet along the cavity axis and reversed upward flow along the side walls was established. This final state was reached after about 40 minutes. Figure 5 shows the observed and calculated temperature and velocity fields in the vertical centre symmetry plane for this configuration.

The overall agreement between calculated and measured characteristics of the flow structure (velocity fields) is very good (Fig.6 top) and the numerically predicted shape of the cold plume is in good agreement with that observed (Fig.5). However, as it can be seen in figures 5 and 6, the measured temperature values are approximately 30%

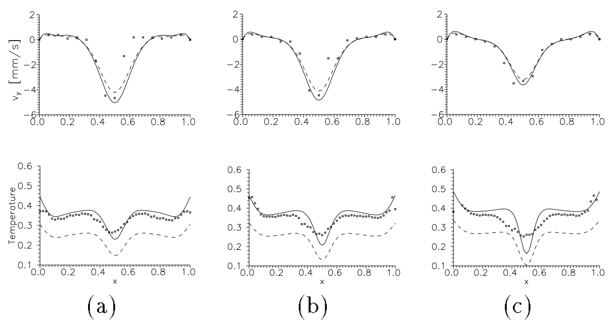

Figure 6: *Comparison of velocity (above) and temperature (below) profiles for the final state at the z=0.5 and (a) y=0.25, (b) y=0.5 and (c) y=0.75. Measured values (symbols), calculated profiles using nominal heat flux (dashed lines) and fitted one (full lines).*

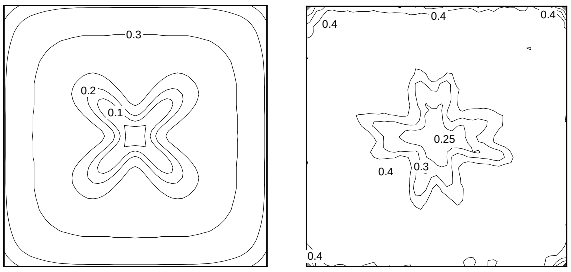

Figure 7: *Calculated (left) and measured (right) non-dimensional temperature distribution underneath the cooled lid (plane y=0.9); water, $Ra = 2.7 \times 10^6$, $T_h = 21^oC$, $T_c = 15.5^oC$, steady state.*

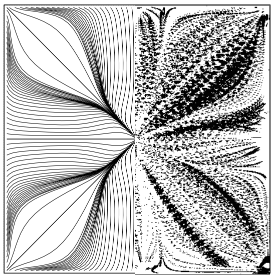

Figure 8: *Calculated (left) and observed (right) particle tracks underneath the cooled lid (plane y=0.95) viewed from above.*

higher than that predicted. It is believed that this is a result of an underestimation of the heat flux through the five non-adiabatic walls in the numerical model. In order to investigate this hypothesis the final (steady) flow state was calculated using FRECON3D. In the several computational runs the TBC on the non-adiabatic walls were step-wise modified so as to give better agreement between the calculated and measured temperature profiles. It was found that such agreement could be obtained (Fig. 6 solid lines) by assuming nearly twice as much heat flux through the side walls as the nominal value calculated from the physical characteristics of the side walls. It would seem that the heat flux along the side walls, which we neglected in equation (4), effectively increases the heat transfer from the outside medium to the fluid. It is worth noting that the velocity field exhibits only a weak dependence on the assumed TBC on the side-walls and for both cases shown in Fig.6 (top) the velocity profiles are practically the same.

The effect of the temperature dependence of the fluid properties (density, viscosity and thermal conductivity) on the overall flow structure was examined. Over the temperature range considered, the viscosity of water shows a substantial variation - about 10% - while the other properties do not vary significantly. In the calculations with and without the temperature dependence of the fluid properties, the differences in the solutions were very small. The maximum values of the flow velocity dropped by less than 2.5% when variable fluid properties are considered, and the flow structure, temperature distribution and velocity profiles showed practically the same form.

Although good agreement has been obtained between the measured and predicted general structure of the flow and thermal fields, there are discrepancies in the fine details of these fields. This is particularly noticeable in the

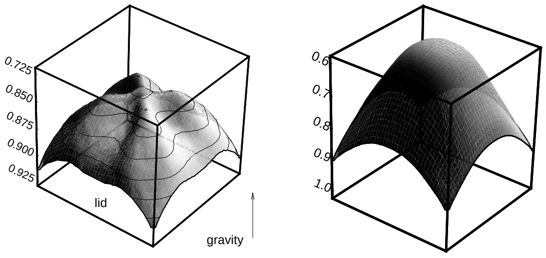

(a) (b)

Figure 9: *Ice formation under the lid of the lid-cooled cavity. Ice surface calculated at 6 min (a) and 60 min (b) after the start of cooling started. The interface is seen from below. $Ra = 3.1 \times 10^6$, $Pr = 13$.*

flow and temperature distributions just below the top lid.

Both the computed and measured temperature distributions (Fig.7) show an eight fold symmetry, but as may be seen the patterns are oriented differently.

In the numerical results, the cubic symmetry of the cavity generates an eight-fold structure of the internal flow (see Fig.8), with apparently closed flow regions.

The calculated streamline starting in the diagonal symmetry plane spirals inwards towards the centre of this plane, where it then crosses over to the central symmetry plane, spirals outwards and eventually returns to the starting position on the diagonal plane. Physically it is possible for a flow pattern with the opposite sequence to develop, that is spiralling inwards in the central plane and outwards on the diagonal plane.

Our present task is to determine if observed differences are due to inappropriately specified temperature boundary conditions at the side walls, or perhaps due to a 'weak' instability of the symmetrical flow structure, which may be easily distorted if some geometrical or thermal disturbances exist.

Preliminary results have indicated that conduction along the thick plexiglas walls is the triggering mechanism to this variation in the fine structural details. This work is currently in progress and will be reported elsewhere.

4.2. Ice growth

The formation of ice has been studied by decreasing the lid temperature to -10^oC. A complicated flow pattern appears after convection starts. This is also manifested in the complex structure of the ice surface (Fig.9a). Similar to the computed initial ice surface, a diamond-like pattern of the ice front has been observed in the experiment.

It was found that the creation of the ice layer at the lid has a stabilising effect on the flow. The diamond shaped pattern of the ice-fluid interface which forms on the lid of the cavity imposes the direction and character of the flow, eliminating the instabilities observed for the pure convection case. There is also a density inversion under the lid which decelerates the main 'jet' and limits the strong generation of vorticity in that region.

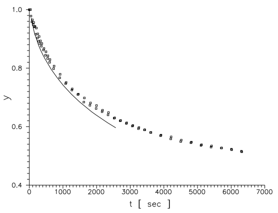

Figure 10: *Measured (symbols) and calculated (line) ice interface growth rate.*

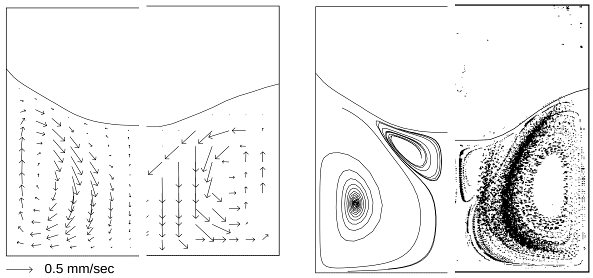

Figure 11: *Calculated (left half) and measured (right half) velocity vectors and particle tracks at the vertical centre plane z=0.5; Ra* $= 3.1 \times 10^6$, $Pr = 13$.

Figure 10 shows the variation of the height of the ice front at the centre of the cavity with time. There is good general agreement between experiment and computations, although as can be seen the numerical model predicted a slightly higher rate of ice growth. This is consistent with the hypothesis that the heat transfer rate in the experiments was higher than estimated and used in the model. This has also been verified in our preliminary investigations of the effects of conduction in the thick plexiglas walls on the fluid structure.

A comparison of the predicted (left) and measured (right) ice/water interface and the associated flow structures can be seen in Fig.11. There is a primary cell which carries hot fluid up the wall to the ice interface, resulting in a cutting back of the outer edges of this interface; water then flows down in the centre of the cavity. Just below the ice in the centre of the cavity there are small counter rotating secondary flows established due to the density extremum of water in this region. This can be clearly seen in the particle tracks shown in Fig.11.

5. CONCLUDING REMARKS

The simultaneous measurement of flow and temperature fields using liquid crystals as tracers allowed a qualitative description to be made of the onset of convection generated under the cooled lid. The numerical results show good quantitative agreement in the velocity fields. The differences found in the details of the flow pattern and temperature fields are believed to result from inappropriately specified TBC on the non-adiabatic walls. The computations showed that heat flux through these walls is underestimated by neglecting heat conduction along the side walls. The simple condition (4) seems to be inadequate in the description of the heat flux for the relatively thick walls used in the present experiment (0.21 of the box size). This has already been confirmed in preliminary simulations of the coupled conduction/convection problem for this particular situation.

The observed differences in the symmetry of the temperature profile close to the lid results in the change of the flow pattern. It has already been found that for the differentially heated cavity (Hiller *et al.* 1990), different flow structures can be obtained depending on thermal boundary conditions defined on the side walls. It would appear to be also the case for the lid-cooled cavity. A number of different flow patterns are possible in the lid-cooled cavity investigated in this paper. The final steady flow which develops is strongly dependent on the 'side' wall thermal boundary conditions and possibly other triggering mechanisms. This is now being investigated.

REFERENCES

Goh, L.P., Leonardi, E. & de Vahl Davis, G. 1988, FRECON3D - Users Manual. A program for the numerical solution of mixed convection in a three- dimensional rectangular cavity, Report 1988/FMT/7, University of New South Wales, Kensington, Australia.

Hiller, W.J., Koch, St., Kowalewski, T.A., de Vahl Davis, G. & Behnia, M. 1990, Experimental and numerical investigation of natural convection in a cube with two heated side walls, in Topological Fluid Mechanics, Proceedings of the IUTAM Symposium, edts. H.K. Moffat & A. Tsinober, pp. 717 - 726, CUP, Cambridge.

Hiller, W.J., Koch, St., Kowalewski, T.A. & Stella, F. 1993, Onset of natural convection in a cube, Int. J. Heat Mass Transfer, vol. 36, pp. 3251-3263.

Leonardi, E. & Reizes, J.A. 1981, Convective Flows in Closed Cavities with Variable Fluid Properties, Chap. 18 in Numerical Methods in Heat Transfer, ed. Lewis, R.W., Morgan, K. and Zienkiewicz, O.C., John Wiley & Sons.

Mallinson, G.D. & de Vahl Davis, G. 1977, Three-dimensional natural convection in a box: a numerical study, J. Fluid Mech., vol. 83, pp. 1-31.

Müller, G., Neumann, G. & Matz, H. 1987, A Two-Rayleigh-Number model of buoyancy-driven convection in vertical melt growth configurations, J. Crystal Growth, vol. 84, pp. 36-49.

Paul, R. 1991, Die Erfassung von Geschwindigkeitsfeldern durch automatische Bewegungsanalyse am Beispiel einer rotierenden Flüssigkeit, Ph.D. thesis in Mitteilungen aus dem MPI Göttingen, No. 102.

Rosenberger, F. & Müller, G. 1983, Interfacial transport in crystal growth, a parametric comparison of convective effects, J. of Crystal Growth, vol. 65, pp. 91-104.

Stella, F., Guj G. & Leonardi, E. 1993, The Rayleigh-Bénard problem in intermediate bounded domains, J. Fluid Mech., vol. 254, pp. 375-400.

Yeoh, G.H. 1993, Natural convection in a solidifying liquid, Ph.D. thesis, University of New South Wales, Kensington, Australia.